Energy Minimization for UAV-Enabled Wireless Power Transfer and Relay Networks

Zhenyao He, *Graduate Student Member, IEEE,* Yukuan Ji, Kezhi Wang, *Senior Member, IEEE,* Wei Xu, *Senior Member, IEEE,* Hong Shen, *Member, IEEE,* Ning Wang, *Member, IEEE,* and Xiaohu You, *Fellow, IEEE*

***Abstract*—In this paper, we consider an unmanned aerial vehicle (UAV)-enabled wireless power transfer (WPT) and relay communication network consisting of a base station (BS), a UAV, and multiple ground users. The UAV acts as both a wireless power transmission source and an uplink communication relay. Specifically, an entire transmission period of the considered system is divided into two stages. In the first stage, the UAV transfers the power to the ground users along a well-optimized flight trajectory and meanwhile the users transmit data to the UAV using the harvested energy. Subsequently, in the second stage, the UAV flies to the vicinity of the BS and forwards the data to the BS. For the purpose of minimizing the energy consumed by the UAV, we jointly optimize the time durations of the two stages, the UAV's transmit powers for WPT and data forwarding, as well as its flight trajectory, subject to the constraints of the quality of service (QoS), the information forwarding, the energy causality, and the mobility of the UAV. The involved optimization problem is non-convex and highly intractable. To this end, we propose an efficient alternating algorithm to iteratively solve two subproblems with respect to the time durations of the two stages and the UAV's transmit powers and trajectory, respectively. The first subproblem has a closed-form optimal solution and the second subproblem is handled by addressing a surrogate convex problem based on the technique of successive convex approximation. Finally, simulation results confirm the superiority of our proposed algorithm.**

***Index Terms*—Unmanned aerial vehicle (UAV), wireless power transfer, mobile relay, trajectory design, joint optimization.**

This work was supported in part by the National Key Research and Development Program 2020YFB1806608; in part by the NSFC under Grants 62022026 and 62211530108; in part by the Fundamental Research Funds for the Central Universities under Grants 2242022K60002 and 2242023K5003; and in part by the Natural Science Foundation of Jiangsu Province under Grant BK20201263. The work of N. Wang is partly supported by the Open Research Fund of State Key Laboratory of Millimeter Waves under Grant K202214. *(Corresponding authors: Wei Xu; Hong Shen.)*

Z. He, W. Xu, and X. You are with the Frontiers Science Center for Mobile Information Communication and Security, National Mobile Communications Research Laboratory, Southeast University, Nanjing 210096, China, and also with the Purple Mountain Laboratories, Nanjing 211111, China (e-mail: {hezhenyao, wxu, xhyu}@seu.edu.cn).

Y. Ji is with the Nanjing Power Supply Company, State Grid Jiangsu Electric Power CO. LTD, Nanjing 210000, China (e-mail: ykjiseu@163.com).

K. Wang is with the Department of Computer Science, Brunel University London, Uxbridge, Middlesex, UB8 3PH, UK (email: kezhi.wang@brunel.ac.uk).

H. Shen is with the National Mobile Communications Research Laboratory, Southeast University, Nanjing 210096, China (e-mail: shhseu@seu.edu.cn).

N. Wang is with the School of Information Engineering, Zhengzhou University, Zhengzhou 450001, China (e-mail: ienwang@zzu.edu.cn).

I. Introduction

With the exponential growth of the number of network-connected devices, various new technologies are becoming the driving force of 5G/6G development. In particular, the upsurge of Internet of Things (IoT) has significantly facilitated the evolution of existing wireless networks [1]–[4]. It is foreseeable that the IoT has a wide range of application scenarios, such as home automation, industrial intelligence, and healthcare, which provides much convenience for human beings [5]. However, achieving the vision of IoT still faces some challenges, one of which is the energy issue. Specifically, the devices of IoT are usually small in size and have finite battery capacity, resulting in extremely limited operation time. Therefore, an efficient energy replenishment solution is urgently required to prolong the worklife of devices and support a sustainable system [6], [7]. Replacing the batteries is the most direct way to recharge energy-constrained devices [8], however, it is costly and inconvenient due to the fact that a great number of devices are distributed over a wide range area which are hard to reach. Alternatively, many studies have pointed out that a more practical method is to let devices harvest energy from surrounding environment. Among various forms of energy sources, including solar, wind, and thermal, ambient radio frequency (RF) signals are considered more suitable for carrying energy to provide low-cost and stable power for devices [8]–[10].

However, the performance of RF-based wireless power transfer (WPT) is fundamentally affected by the severe propagation loss, including path loss, fading, and attenuation [11]. In particular, for a long-distance WPT, the energy source must increase the transmit power to ensure sufficient received power at receiving nodes to perform energy harvesting (EH), which reduces the energy efficiency [12]–[14] of the system and violates the principle of green communications. On the other hand, for traditional RF-based WPT systems, the energy source, e.g., a base station (BS) or other entity, has a fixed physical location and is inconvenient for dynamic deployment. Therefore, to provide ubiquitous energy access for massive devices, energy sources must be densely deployed, which greatly increases the cost of system construction and hinders the development of WPT systems [11]. In order to mitigate the shortcomings of conventional RF-based WPT systems, researchers have proposed various methods to improve the efficiency of WPT. For example, multi-antenna beamforming designs for efficient WPT have been investigated in [8], [15]–[18]. The works [19], [20] took into account the multiuser

This article has been accepted for publication in a future issue of this journal, but has not been fully edited. Content may change prior to final publication. Citation information: DOI10.1109/JIOT.2023.3281584, IEEE Internet of Things Journal

scheduling scheme for the sake of improving the power transfer efficiency.

Recently, unmanned aerial vehicles (UAVs) have been employed in a wide range of applications to assist wireless networks [21]–[25]. In particular, due to the enlarged coverage and better communication channel, e.g., a short range line-of-sight (LoS) link, brought by the UAV, it is shown in the literature [21], [22], [26]–[31] that the UAV-aided relay can significantly improve the wireless communication performance, especially when the distant ground nodes do not have reliable direct links. Moreover, compared to the conventional static relays with fixed location, the UAV-assisted relay technique offers new opportunities for performance enhancement due to its flexible mobility, meanwhile requiring a careful trajectory design. For example, the authors in [27] investigated a point-to-point wireless communication relay system, where a mobile UAV forwarded information from the source to the destination. By jointly optimizing the UAV's trajectory and power allocations of the source and the UAV, a significant throughput enhancement over the traditional static relays is achieved. A similar joint optimization problem in terms of outage probability minimization was further considered in [28]. In [29], the authors investigated the joint optimization of blocklength allocation and UAV location to minimize the decoding error probability in UAV-relaying communications. In addition, the authors in [30], [31] studied the enhancement of multicell edge communications by a mobile UAV relay. By properly optimizing the UAV mobility management, e.g., trajectory and velocity, the rate of the edge users is dramatically increased. Besides, the multi-UAV cooperation [32] and security performance [33] of UAV-relaying system have also been addressed.

On the other hand, UAVs are also considered promising to be integrated into WPT systems as energy sources to compensate for the limitations of traditional sources [11], [34]–[40]. The advantages of deploying UAV for WPT mainly lie in the following two aspects. On the one hand, due to the high flight altitude, UAVs make it easier to shorten the distance and construct LoS links with ground devices, thus significantly reducing the pass loss and improving the efficiency of WPT. On the other hand, owing to the mobility, UAVs can dynamically adjust their positions according to the distribution of devices, which can help realize the WPT in a flexible manner. In [11], the authors studied the problem of UAV's trajectory design in a UAV-enabled WPT system. It was shown that the power transfer efficiency can be greatly improved with the assistance of UAV. From the fairness perspective, the authors in [35] considered maximizing the minimum harvested energy among all ground nodes by jointly designing the trajectory and directional antenna orientation of the UAV. The problems of throughput maximization and energy minimization for a UAV-enabled WPT system were investigated in [36] and [37], respectively, where the UAV acts as a WPT transmitter and a data collector. Further, taking the timeliness and covertness of data collection into account, the authors in [38] optimized the transmit power and durations in a UAV-aided WPT IoT network. In addition, the UAV-assisted wireless powered mobile edge computation (MEC) systems were investigated in [39], [40]. However, note that the signal processing capability at the UAV is finite due to its limited carrying capacity. Therefore, it is still necessary for the UAV to forward data to a BS that has a much higher computational capability, especially when the task exceeds the UAV's processing limits. This motivates us to investigate a new scenario, where a dual-functional UAV acts as both a WPT transmitter and a mobile relay. Such a scenario yields a more challenging design problem and the algorithms proposed in existing works cannot be straightforwardly employed to address it, since they do not consider the incorporation of WPT and data forwarding functions.

Based on the above discussion, this paper investigates a UAV-enabled WPT and relay network, in which the UAV serves as a wireless power transmission source and an uplink relay simultaneously. The main contributions of this paper are summarized as follows.

- In order to complete the WPT and wireless relaying, we consider that a transmission period is divided into two stages. In the first stage, the UAV charges the ground users via RF WPT and receives the uplink data from the users along a well-optimized flight trajectory. Then, in the second stage, the UAV flies to the BS and forwards the collected multiuser data to the BS.
- Under this setup, to minimize the energy consumed by the UAV, we formulate a joint optimization problem with respect to the time durations of the two stages and the transmit powers and trajectory of the UAV, subject to the quality of service (QoS) constraints of the ground users, the causal constraints for both EH and data forwarding, and the mobility constraints of the UAV.
- The considered optimization is a challenging non-convex problem with highly coupled variables and complicated constraints. To address it, we develop an alternating optimization-based method. First, for the subproblem with respect to time durations, we derive the optimal solution in closed form. Then, for the intractable subproblem with respect to the UAV's powers and trajectory, we employ the technique of successive convex approximation (SCA) to handle the non-convexities brought by the complicated constraints, where a locally approximate surrogate convex problem is solved in each iteration.

Simulation results confirm the effectiveness of our proposed algorithm compared to other benchmark schemes.

The rest of this paper is organized as follows. Section II presents the system model of the considered UAV-enabled WPT and relay network and formulates the joint optimization problem. In Section III, an iterative algorithm is proposed to handle the complicated optimization problem. Numerical results are presented in Section IV. Finally, this paper is concluded in Section V.

Notations: Boldface lower-case letters denote vectors. $(\cdot)^T$ and $(\cdot)^H$ represent the transpose and the Hermitian transpose operations, respectively. $\|\cdot\|$ denotes the ℓ_2 norm of a vector. $|\cdot|$ stands for the absolute value of a scalar. $\mathcal{O}(\cdot)$ stands for the big-O computational complexity notation.

This article has been accepted for publication in a future issue of this journal, but has not been fully edited. Content may change prior to final publication. Citation information: DOI10.1109/JIOT.2023.3281584, IEEE Internet of Things Journal

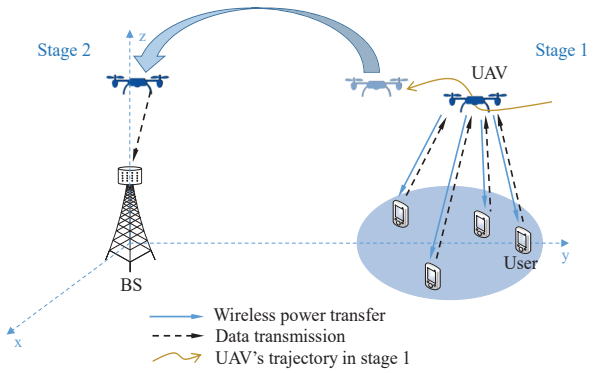

Fig. 1. The considered UAV-enabled WPT and relay network.

II. System Model and Problem Formulation

A. System Model

We consider a UAV-enabled WPT and relay communication network consisting of an L-antenna BS, a single-antenna fixed-wing UAV, and a set $\mathcal{K} = \{1, \cdots, K\}$ of single-antenna users that are distributed far away from the BS, as shown in Fig. 1. These involved users can be all kinds of cell-edge IoT devices, such as sensors and actuators, and perform different kinds of tasks, such as environmental monitoring and edge computing. It is assumed that the ground users have limited power resource and are capable of gaining energy through EH. To handle the energy-limitations of these IoT devices, a UAV is introduced and acts as an RF wireless power transmission source to provide energy supplies. The own energy of each user is used to collect data from the environment or conduct the edge computing and the harvested energy is used to offload its data to the UAV. On the other hand, it is assumed that the direct communication links between the BS and the users are neglected due to the large distance between them. Thus, the UAV meanwhile works as an uplink mobile relay to forward the communication data from the users to the BS.

In the considered system, for the purpose of accomplishing the simultaneous functionalities of WPT and communication relaying, a complete transmission period is divided into two stages of length t_1 and t_2, respectively. During the first stage, the UAV flies above the ground users along a well-designed trajectory and charges the users through RF signals. At the same time, the users transmit data to the UAV utilizing the harvested energy. While during the second stage, the UAV flies to a predetermined location near the BS and forwards the data to the BS[1]. Without loss of generality, we consider a three-dimensional (3D) Cartesian coordinate system, where the BS and the users are located on the ground with zero altitude. The fixed horizontal locations of the BS and user k are denoted as $\boldsymbol{b} = (x_b, y_b)$ and $\boldsymbol{e}_k = (x_k, y_k)$, $k \in \mathcal{K}$, respectively. The UAV flies horizontally at fixed height H. Moreover, we assume that the locations of the BS and the users are known to the UAV for designing trajectory [11]. The detailed descriptions of the two stages are given as follows.

1) Stage 1 - Power Transfer and Data Collection: During the first stage, the UAV transfers power and receives data from the users simultaneously in frequency division duplex (FDD) mode [18]. Further, in order to allow each user to send data to the UAV and suppress the interference, the users are assumed to associate with the UAV in a time division multiple access (TDMA) manner [18], [40]. Specifically, the finite duration t_1 can be discretized into N equal-length time intervals. N is large enough such that the location of the UAV is approximately unchanged during each time interval, which is denoted as $\boldsymbol{u}[n] = (x[n], y[n])$ for $n \in \{1, \cdots, N\} \triangleq \mathcal{N}$. Each time interval with length $\frac{t_1}{N}$ is further split into K time slots for K users sequentially associating with the UAV, each of which lasts for $\tau = \frac{t_1}{NK}$ seconds.

Let $\boldsymbol{u}_0$ denote the the predetermined initial point of the UAV trajectory during the first stage. Assuming that we use a fixed-wing UAV which cannot hover in a fixed position, apart from the maximum flight speed limit, there also exists a minimum flight speed constraint [21]. Then, the mobility constraints of the UAV can be modeled as

$$\boldsymbol{u}[1] = \boldsymbol{u}_0, \tag{1}$$

$$V_{\min} \le v[n] \le V_{\max}, \ n = 1, \cdots, N-1, \tag{2}$$

where

$$v[n] \triangleq \frac{\|\boldsymbol{u}[n+1] - \boldsymbol{u}[n]\|}{t_1/N} \tag{3}$$

denotes the average flight speed during the n-th time interval, $V_{\min}$ and $V_{\max}$ represent the minimum and the maximum flight speed of the UAV, respectively.

We consider an open-air environment and assume that the wireless channels between the UAV and the users are dominated by the LoS links due to the high flight altitude of the UAV [11], [21], [40]. Without loss of generality, we consider the n-th time interval. Adopting the free-space path-loss model in [21], the channel power gain between the UAV and user k is expressed as

$$\begin{aligned} h_{uk}[n] &= \alpha_0 d_{uk}^{-2}[n] \\ &= \frac{\alpha_0}{H^2 + \|\boldsymbol{u}[n] - \boldsymbol{e}_k\|^2}, \end{aligned} \tag{4}$$

where α_0 is the reference channel power at $d_0 = 1$ m and $d_{uk}[n]$ denotes the distance between the UAV and user k. Further, following [8], [40], we consider a linear EH model at each user. Mathematically, let $p_1[n] \le P_{\max}$ denote the transmit power of the UAV when charging the users during the n-th time interval, where $P_{\max}$ is the allowed maximum power. With the channel power gain $h_{uk}[n]$, the energy harvested by user k during the n-th time interval is given by [40]

$$E_k^{\mathrm{EH}}[n] = \eta p_1[n] h_{uk}[n] \frac{t_1}{N}, \tag{5}$$

where $0 < \eta \le 1$ represents the energy conservation efficiency.

[1]Apart from the aforementioned two stages, there exists another intermediate process, where the UAV flies from the final location of the first stage to the vicinity of the BS to proceed with the second stage. Note that during this intermediate stage, the UAV is far away from both the users and the BS, such that it does not perform the tasks of WPT nor communication and works in a predetermined flight-only strategy. As a result, we ignore the impacts of this flight process and only focus on the design of the other two stages where the UAV is close to the BS or the users.

By leveraging the harvested energy, each user offloads its data to the UAV through the uplink communication. Denoting the constant transmission power of user k by P_k^{user}, the transmission data rate is correspondingly given by

$$R_k[n] = B\log_2\left(1+\frac{P_k^{\text{user}}h_{uk}[n]}{\sigma_u^2}\right),\ \forall k\in\mathcal{K}, \tag{6}$$

where B stands for the communication bandwidth and σ_u^2 represents the variance of the additive white Gaussian noise (AWGN) at the UAV. Assuming that the energy consumed for uplink offloading at each user is obtained from EH only, the energy consumed by each user for data transmission cannot exceed the energy that it has collected. This results in a group of energy causality constraints as follows:

$$n\tau P_k^{\text{user}} \le \sum_{i=1}^{n} E_k^{\text{EH}}[i],\ \forall k\in\mathcal{K}, \forall n\in\mathcal{N}. \tag{7}$$

In (7), the constraint with arbitrary (k,n) guarantees that user k can successfully offload data to the UAV during the previous n time slots by employing the harvested energy.

2) Stage 2 - Communication Relaying: During the second stage of length t_2, the UAV flies near the BS and forwards the data to the BS with transmit power p_2. Since the BS is located in a fixed location, the speed and trajectory of the UAV during this stage can be predetermined and are no longer needed to be optimized. As such, when communicating with the BS, we assume that the UAV files in a circular trajectory with a constant speed and the distance between the UAV and the receive antenna array at the BS, denoted as d_{ub}, remains unchanged. Let D be this constant distance. The channel power gain between the UAV and the BS is similarly evaluated as

$$h_{ub} = \alpha_0 d_{ub}^{-2} = \frac{\alpha_0}{D^2}. \tag{8}$$

On the other hand, let us define the small-scale fading channel between the UAV and the BS by $\boldsymbol{g}\in\mathbb{C}^{L\times 1}$. The BS adopts a receive beamforming vector $\boldsymbol{w}\in\mathbb{C}^{L\times 1}$ to recover the data from the received signal. As a result, the data rate of the UAV-BS link is obtained by

$$R_{ub} = B\log_2\left(1+\frac{p_2 h_{ub}|\boldsymbol{g}^H\boldsymbol{w}|^2}{\sigma_b^2\boldsymbol{w}^H\boldsymbol{w}}\right), \tag{9}$$

where σ_b^2 represents the variance of the AWGN at the BS. To maximize the receive signal-to-noise ratio (SNR), the maximum ratio combining (MRC) strategy is adopted at the BS with $\boldsymbol{w}=\frac{\boldsymbol{g}}{\|\boldsymbol{g}\|}$. Substituting $\boldsymbol{w}=\frac{\boldsymbol{g}}{\|\boldsymbol{g}\|}$ into the rate in (9) yields

$$R_{ub} = B\log_2\left(1+\frac{p_2 h_{ub}\|\boldsymbol{g}\|^2}{\sigma_b^2}\right). \tag{10}$$

Also, assuming that there only exists a LoS path between the BS and the UAV due to the high flight altitude, we thus have $\|\boldsymbol{g}\|^2 = L$.

Moreover, to ensure that all the data received from the users can be successfully forwarded to the BS, we introduce the following information constraint

$$R_{ub}t_2 \ge \sum_{k=1}^{K}\sum_{n=1}^{N} R_k[n]\tau, \tag{11}$$

which couples the designs of the considered two stages.

B. UAV Energy Consumption

In this part, we character the total energy consumption model at the UAV, which includes the energy consumed to charge the users, the energy used for communicating with the BS, and the propulsion energy used to maintain the flight.

1) Energy Consumption for Power Transfer and Communication: Recall that in the processes of charging users and communicating with the BS, the UAV's transmit powers are $\{p_1[n]\}_{n=1}^N$ and p_2, respectively. Then, the consumed energy for WPT and communication is related to the transmit powers and time durations of these two stages and is given by

$$E_u^1 = \sum_{n=1}^{N} p_1[n]\frac{t_1}{N} + p_2 t_2. \tag{12}$$

2) Energy Consumption for Flight: As for the propulsion energy consumption for the flight, we consider a simplified model commonly applied in existing works [24], [40]. Specifically, in the first stage, the propulsion energy consumed in the n-th time interval is determined by the UAV's velocity $v[n]$ and it is given by [24]

$$\begin{aligned} E_u^{\text{fly}}[n] &= \kappa_f (v[n])^2 \\ &= \frac{0.5MN}{t_1}\|\boldsymbol{u}[n+1]-\boldsymbol{u}[n]\|^2 \end{aligned} \tag{13}$$

where $\kappa_f \triangleq 0.5M\frac{t_1}{N}$ and M denotes the mass of the UAV. In the second stage, the UAV performs a uniform circular motion near the top of the BS, which consumes a constant propulsion power, denoted by P_{c}, and the corresponding flight energy consumption is $P_{\text{c}}t_2$.

According to the above analysis, we obtain the total energy consumption of the UAV during a complete transmission period by

$$E_u^{\text{total}} = \underbrace{\sum_{n=1}^{N} p_1[n]\frac{t_1}{N}}_{\text{WPT}} + \underbrace{p_2 t_2}_{\text{communication}} + \underbrace{\sum_{n=1}^{N-1} E_u^{\text{fly}}[n] + P_{\text{c}}t_2}_{\text{flight}}. \tag{14}$$

C. Problem Formulation

In this paper, the design goal is to minimize the total energy consumption of the UAV during the whole transmission period, by jointly optimizing the time durations of two stages, $\boldsymbol{T} \triangleq \{t_1, t_2\}$, the transmit powers of UAV at two stages, $\boldsymbol{P} \triangleq \{p_1[n], p_2,\ \forall n \in \mathcal{N}\}$, and the UAV's trajectory,

This article has been accepted for publication in a future issue of this journal, but has not been fully edited. Content may change prior to final publication. Citation information: DOI10.1109/JIOT.2023.3281584, IEEE Internet of Things Journal

$\boldsymbol{U} \triangleq \{\boldsymbol{u}[n],\ \forall n \in \mathcal{N}\}$. Accordingly, the optimization problem is formulated as

$$\begin{aligned}
\underset{\boldsymbol{U},\boldsymbol{T},\boldsymbol{P}}{\text{minimize}} \quad & E_u^{\text{total}} && (15)\\
\text{subject to} \quad & \sum_{n=1}^{N} R_k[n]\tau \geq r_k,\ \forall k \in \mathcal{K}, && (15a)\\
& n\tau P_k^{\text{user}} \leq \sum_{i=1}^{n} E_k^{\text{EH}}[i],\ \forall k \in \mathcal{K}, \forall n \in \mathcal{N}, && (15b)\\
& R_{ub} t_2 \geq \sum_{k=1}^{K}\sum_{n=1}^{N} R_k[n]\tau, && (15c)\\
& \boldsymbol{u}[1] = \boldsymbol{u}_0, && (15d)\\
& V_{\min} \leq v[n] \leq V_{\max},\ n = 1, \cdots, N-1. && (15e)
\end{aligned}$$

The objective function of problem (15) represents the total energy consumption at the UAV. The constraints in (15a) stand for the communication QoS constraints of all the users, where r_k is the total bits of data at user k that needs to be transmitted. Energy causality constraints (15b) ensure that the transmit energy consumed at each user cannot exceed its harvested energy. The information constraint in (15c) guarantees that all the data received by the UAV can be successfully forwarded to the BS. Mobility constraints (15d) and (15e) are used for limiting the initial point and the flight speed of the UAV.

Note that in problem (15) the optimization variables $\{\boldsymbol{U}, \boldsymbol{T}, \boldsymbol{P}\}$ are tightly coupled with each other and the involved constraints have complicated forms. These make problem (15) non-convex and highly intractable, whose optimal solution is challenging to be obtained in general.

III. Joint Time Duration, Transmit Power, and Trajectory Optimization

In this section, we provide an efficient algorithm to handle problem (15) by optimizing the time durations and the transmit powers as well as the trajectory of the UAV in an alternating manner. Specifically, with the fixed $\{\boldsymbol{U}, \boldsymbol{P}\}$, the optimal solution of $\boldsymbol{T}$ is derived in closed form. Given $\boldsymbol{T}$, we update $\{\boldsymbol{U}, \boldsymbol{P}\}$ by solving a locally approximate convex problem based on the technique of SCA.

A. Time Duration Optimization

We first focus on the time duration optimization with fixed UAV trajectory and transmit powers. By removing the constraints that are irrelevant to $\boldsymbol{T}$ in (15), we reformulate the subproblem with respect to $\boldsymbol{T}$ as

$$\begin{aligned}
\underset{t_1 \geq 0, t_2 \geq 0}{\text{minimize}} \quad & \bar{p}_1 t_1 + (p_2 + P_{\text{c}}) t_2 \\
& + \sum_{n=1}^{N-1} \frac{0.5MN}{t_1} \|\boldsymbol{u}[n+1] - \boldsymbol{u}[n]\|^2 \\
\text{subject to} \quad & \sum_{n=1}^{N} R_k[n] \frac{t_1}{NK} \geq r_k,\ \forall k \in \mathcal{K}, \\
& R_{ub} t_2 \geq \sum_{k=1}^{K}\sum_{n=1}^{N} R_k[n] \frac{t_1}{NK}, \\
& V_{\min} \leq \frac{\|\boldsymbol{u}[n+1] - \boldsymbol{u}[n]\|}{t_1/N} \leq V_{\max}, \\
& \qquad\qquad n = 1, \cdots, N-1, \qquad (16)
\end{aligned}$$

where $\bar{p}_1 \triangleq \sum_{n=1}^{N} p_1[n]/N$. Focusing on this problem, it is easily verified that the objective function is convex for $t_1 > 0$ and all the constraints can be transformed into linear constraints with respect to $\boldsymbol{T}$. This confirms that (16) is a convex problem and its globally optimal solution can be found, e.g., via the interior point method [41] or the off-the-shelf convex optimization tools such as CVX [42]. In fact, the optimal solution of problem (16) can be directly obtained in closed form with lower computational complexity, which will be shown in the following proposition.

Proposition 1: The optimal solution of problem (16) takes the form:

$$\begin{aligned}
t_1^* &= \begin{cases} \max_{t_1}, & \text{if } \max_{t_1} \leq \tilde{t}_1, \\ \tilde{t}_1, & \text{if } \max_{t_1} > \tilde{t}_1 \text{ and } \min_{t_1} \leq \tilde{t}_1, \\ \min_{t_1}, & \text{if } \min_{t_1} > \tilde{t}_1, \end{cases} \\
t_2^* &= \frac{\sum_{k=1}^{K}\sum_{n=1}^{N} R_k[n]}{R_{ub} NK} t_1^*. \qquad (17)
\end{aligned}$$

where the definitions of $\tilde{t}_1$, $\min_{t_1}$, and $\max_{t_1}$ are respectively given by

$$\begin{aligned}
\tilde{t}_1 &\triangleq \sqrt{\frac{MN \sum_{n=1}^{N-1} \|\boldsymbol{u}[n+1] - \boldsymbol{u}[n]\|^2}{2\left(\bar{p}_1 + \frac{p_2 + P_{\text{c}}}{R_{ub} NK} \sum_{k=1}^{K}\sum_{n=1}^{N} R_k[n]\right)}}, \\
\min_{t_1} &\triangleq \max(\text{lb}_0, \text{lb}_1, \cdots, \text{lb}_{N-1}), \\
\max_{t_1} &\triangleq \min(\text{ub}_1, \cdots, \text{ub}_{N-1}). \qquad (18)
\end{aligned}$$

The detailed calculations of $\{\text{lb}_n\}_{n=0}^{N-1}$ and $\{\text{ub}_n\}_{n=1}^{N-1}$ are given by (42)–(44) in Appendix A.

Proof: Please see Appendix A. ■

B. UAV Transmit Power and Trajectory Optimization

In this part, we perform the optimization to the transmit powers and the trajectory of the UAV. Specifically, given

$\boldsymbol{T}$, the corresponding subproblem with respect to $\{\boldsymbol{U}, \boldsymbol{P}\}$ is formulated as

$$\begin{aligned} \underset{\substack{\boldsymbol{U},\{P_{\max}\geq p_1[n]\geq 0\},\\ p_2\geq 0}}{\text{minimize}} \quad & \sum_{n=1}^{N} p_1[n]\frac{t_1}{N} + p_2 t_2 \\ & + \sum_{n=1}^{N-1} \frac{0.5MN}{t_1}\|\boldsymbol{u}[n+1]-\boldsymbol{u}[n]\|^2 \\ \text{subject to} \quad & (15a)-(15e). \end{aligned} \tag{19}$$

Different from (16), the problem in (19) is more challenging to solve due to the non-convex constraints. To handle this issue, we consider transforming these non-convex constraints into approximate convex forms and iteratively solving the surrogate problem based on the technique of SCA.

Firstly, we focus on the QoS constraints in (15a). By substituting the channel formulation of (4) into (6), we rewrite the communication rate of user k during the n-th time interval, i.e., $R_k[n]$, as

$$R_k[n] = B\log_2\left(1+\frac{\alpha_0 P_k^{\text{user}}}{\sigma_u^2(H^2+\|\boldsymbol{u}[n]-\boldsymbol{e}_k\|^2)}\right), \tag{20}$$

which is not concave with respect to $\boldsymbol{u}[n]$. To address this issue, we exploit the convexity of the function $f(x) \triangleq \log_2(1+\frac{A}{x})$ for arbitrary $A>0$, which can be verified by checking the second-order derivatives, to lower bound $R_k[n]$ by its first-order Taylor expansion [43]. More precisely, since $R_k[n]$ is convex with respect to $\|\boldsymbol{u}[n]-\boldsymbol{e}_k\|^2$, in the l-th iteration we have the following lower bound:

$$\begin{aligned} R_k[n] \geq & -a_k^{(l-1)}[n](\|\boldsymbol{u}[n]-\boldsymbol{e}_k\|^2 - \|\boldsymbol{u}^{(l-1)}[n]-\boldsymbol{e}_k\|^2) \\ & + b_k^{(l-1)}[n] \\ \triangleq & \ \underline{R}_k[n], \end{aligned} \tag{21}$$

where the superscript $(l-1)$ represents the iteration index, and

$$a_k^{(l-1)}[n] = \frac{\frac{BP_k\alpha_0\sigma^2}{[\sigma^2(H^2+\|\boldsymbol{u}^{(l-1)}[n]-\boldsymbol{e}_k\|^2)]^2}\log_2 e}{1+\frac{P_k\alpha_0}{\sigma^2(H^2+\|\boldsymbol{u}^{(l-1)}[n]-\boldsymbol{e}_k\|^2)}} \geq 0, \tag{22}$$

$$b_k^{(l-1)}[n] = B\log_2\left(1+\frac{P_k\alpha_0}{\sigma^2(H^2+\|\boldsymbol{u}^{(l-1)}[n]-\boldsymbol{e}_k\|^2)}\right), \tag{23}$$

with $\boldsymbol{u}^{(l-1)}[n]$ being the optimal solution to $\boldsymbol{u}[n]$ obtained in the $(l-1)$-th iteration. Note that the lower bound $\underline{R}_k[n]$ in (21) is concave with respect to $\boldsymbol{u}[n]$ since $a_k^{(l-1)}[n]$ is nonnegative. Thereby, by invoking (21) for all $n \in \mathcal{N}$, we obtain a set of convex subsets of the non-convex constraints in (15a) as

$$C_1: \quad \sum_{n=1}^{N} \underline{R}_k[n]\frac{t_1}{NK} \geq r_k, \ \forall k \in \mathcal{K}. \tag{24}$$

Next, we deal with the non-convex constraints in (15b). By plugging (5), this group of constraints becomes

$$\begin{aligned} \frac{nP_k^{\text{user}}}{\eta K} \leq & \sum_{i=1}^{n} p_1[i]h_{uk}[i], \\ = & \sum_{i=1}^{n} \frac{\alpha_0 p_1[i]}{H^2+\|\boldsymbol{u}[i]-\boldsymbol{e}_k\|^2}, \ \forall k \in \mathcal{K}, \ \forall n \in \mathcal{N}. \end{aligned} \tag{25}$$

In general, the fractional forms in (25) are challenging to be handled. Fortunately, due to the fact that $p_1[n] \geq 0$, we can denote $q_1[n] \triangleq \sqrt{p_1[n]}, \ \forall n \in \mathcal{N}$, and transform $p_1[i]h_{uk}[i]$ into

$$p_1[i]h_{uk}[i] = \frac{\alpha_0 q_1^2[i]}{H^2+\|\boldsymbol{u}[i]-\boldsymbol{e}_k\|^2}. \tag{26}$$

Note that this belongs to a quadratic-over-linear function $f(x,y) \triangleq \frac{x^2}{y}$, which is jointly convex with respect to x and $y>0$ [41]. We thus lower bound it by exploiting the first-order Taylor expansion on $q_1[i]$ and $H^2+\|\boldsymbol{u}[i]-\boldsymbol{e}_k\|^2$ as

$$\begin{aligned} & \frac{\alpha_0 q_1^2[i]}{H^2+\|\boldsymbol{u}[i]-\boldsymbol{e}_k\|^2} \\ & \geq c_k^{(l-1)}[i]q_1[i] - d_k^{(l-1)}[i](H^2+\|\boldsymbol{u}[i]-\boldsymbol{e}_k\|^2) \\ & \triangleq \underline{h}_{uk}[i], \end{aligned} \tag{27}$$

where

$$c_k^{(l-1)}[i] = \frac{2\alpha_0 q_1^{(l-1)}[i]}{H^2+\|\boldsymbol{u}^{(l-1)}[i]-\boldsymbol{e}_k\|^2}, \tag{28}$$

$$d_k^{(l-1)}[i] = \alpha_0\left(\frac{q_1^{(l-1)}[i]}{H^2+\|\boldsymbol{u}^{(l-1)}[i]-\boldsymbol{e}_k\|^2}\right)^2 \geq 0, \tag{29}$$

with $q_1^{(l-1)}[i] = \sqrt{p_1^{(l-1)}[i]}$ being calculated based on the solution obtained in the $(l-1)$-th iteration. The nonnegative $d_k^{(l-1)}[i]$ guarantees that $\underline{h}_{uk}[i]$ is a concave lower bound. Therefore, by performing the similar procedure to each $p_1[i]h_{uk}[i]$, (25) can be replaced with the following convex approximation as

$$C_2: \quad \frac{nP_k^{\text{user}}}{\eta K} \leq \sum_{i=1}^{n} \underline{h}_{uk}[i], \ \forall k \in \mathcal{K}, \ \forall n \in \mathcal{N}. \tag{30}$$

To proceed, we concentrate on the constraint in (15c). Recall that $R_k[n]$ is convex with respect to $\|\boldsymbol{u}[n]-\boldsymbol{e}_k\|^2$, which, however, is not convex to $\boldsymbol{u}[n]$. To handle this issue, we introduce a group of auxiliary optimization variables, $\omega_k[n]>0, \ \forall k \in \mathcal{K}, \ \forall n \in \mathcal{N}$, and rewrite constraint (15c) equivalently as the following two separate constraints:

$$R_{ub}t_2 \geq \sum_{k=1}^{K}\sum_{n=1}^{N} \log_2\left(1+\frac{1}{\omega_k[n]}\right)\frac{t_1}{NK}, \tag{31}$$

$$\frac{1}{\omega_k[n]} \geq \frac{\alpha_0 P_k^{\text{user}}}{\sigma_u^2(H^2+\|\boldsymbol{u}[n]-\boldsymbol{e}_k\|^2)}, \ \forall k \in \mathcal{K}, \ \forall n \in \mathcal{N}, \tag{32}$$

where $\frac{1}{\omega_k[n]}$ can be interpreted as a copy of the signal-to-noise ratio in $R_k[n]$. The equivalence is established in the sense that the feasible range of $\boldsymbol{U}$ restricted by (31) and (32) keeps the same as that limited by (15c). It is easily seen that the constraint in (31) is already convex and it remains to deal with the non-convex (32). To do this, by taking the inverse of both sides, we first convert (32) to

$$\omega_k[n] \leq \frac{\sigma_u^2(H^2+\|\boldsymbol{u}[n]-\boldsymbol{e}_k\|^2)}{\alpha_0 P_k^{\text{user}}}, \ \forall k \in \mathcal{K}, \ \forall n \in \mathcal{N}. \tag{33}$$

This article has been accepted for publication in a future issue of this journal, but has not been fully edited. Content may change prior to final publication. Citation information: DOI10.1109/JIOT.2023.3281584, IEEE Internet of Things Journal

Then, for the convex function $\|\boldsymbol{u}[n]-\boldsymbol{e}_k\|^2$, exploiting the first-order Taylor expansion yields

$$\begin{aligned}\|\boldsymbol{u}[n]-\boldsymbol{e}_k\|^2 &\geq \|\boldsymbol{u}^{(l-1)}[n]-\boldsymbol{e}_k\|^2 \\ &\quad + 2(\boldsymbol{u}^{(l-1)}[n]-\boldsymbol{e}_k)^T(\boldsymbol{u}[n]-\boldsymbol{u}^{(l-1)}[n]) \\ &\triangleq \underline{u}_k[n]. \end{aligned} \tag{34}$$

Combining (33) and (34), we have found the convex approximations of constraint (32) as

$$\omega_k[n] \leq \frac{\sigma_u^2(H^2+\underline{u}_k[n])}{\alpha_0 P_k^{\text{user}}},\ \forall k\in\mathcal{K},\ \forall n\in\mathcal{N}. \tag{35}$$

Consequently, (15c) can be replaced by two convex constraints given by

$$C_3:\quad (31) \text{ and } (35). \tag{36}$$

Finally, the considered minimum flight speed constraints in (15e) is non-convex. To tackle this issue, we perform the first-order two-dimensional Taylor expansion to $\|\boldsymbol{u}[n+1]-\boldsymbol{u}[n]\|$, which yields

$$\begin{aligned}&\|\boldsymbol{u}[n+1]-\boldsymbol{u}[n]\| \\ &\geq \|\boldsymbol{u}^{(l-1)}[n+1]-\boldsymbol{u}^{(l-1)}[n]\| \\ &\quad + \frac{(\boldsymbol{u}^{(l-1)}[n+1]-\boldsymbol{u}^{(l-1)}[n])^T}{\|\boldsymbol{u}^{(l-1)}[n+1]-\boldsymbol{u}^{(l-1)}[n]\|}(\boldsymbol{u}[n+1]-\boldsymbol{u}^{(l-1)}[n+1]) \\ &\quad + \frac{(\boldsymbol{u}^{(l-1)}[n]-\boldsymbol{u}^{(l-1)}[n+1])^T}{\|\boldsymbol{u}^{(l-1)}[n+1]-\boldsymbol{u}^{(l-1)}[n]\|}(\boldsymbol{u}[n]-\boldsymbol{u}^{(l-1)}[n]) \\ &\triangleq \underline{d}[n]. \end{aligned} \tag{37}$$

The derived linear bound $\underline{d}[n]$ is jointly convex with respect to $\boldsymbol{u}[n+1]$ and $\boldsymbol{u}[n]$. Applying this result, the constraints in (15e) can be replaced with

$$\begin{aligned}C_4:\quad &\frac{\underline{d}[n]}{t_1/N}\geq V_{\min},\ n=1,\cdots,N-1, \\ &\frac{\|\boldsymbol{u}[n+1]-\boldsymbol{u}[n]\|}{t_1/N}\leq V_{\max},\ n=1,\cdots,N-1. \end{aligned} \tag{38}$$

Arming with these obtained convex approximations, we have successfully converted the non-convex constraints in problem (19) into convex ones by introducing lower bound $\underline{R}_k[n]$, lower bound $\underline{h}_{uk}[n]$, lower bound $\underline{u}_k[n]$, and lower bound $\underline{d}[n]$, respectively. In this way, in the l-th iteration, a convex surrogate problem of (19) is given by

$$\begin{aligned}\underset{\boldsymbol{U},\boldsymbol{V},\boldsymbol{Q},p_2}{\text{minimize}}\quad &\sum_{n=1}^{N} q_1^2[n]\frac{t_1}{N}+p_2t_2 \\ &+\sum_{n=1}^{N-1}\frac{0.5MN}{t_1}\|\boldsymbol{u}[n+1]-\boldsymbol{u}[n]\|^2 \\ \text{subject to}\quad &C_1,C_2,C_3,C_4, \\ &\boldsymbol{u}[1]=\boldsymbol{u}_0, \end{aligned} \tag{39}$$

where $\boldsymbol{Q}\triangleq\{0\leq q_1[n]\leq\sqrt{P_{\max}},\ \forall n\in\mathcal{N}\}$ and $\boldsymbol{V}\triangleq\{\omega_k[n]\geq 0,\ \forall k\in\mathcal{K},\ n\in\mathcal{N}\}$. The optimal solution of this convex problem can be readily found by using CVX toolbox [42]. Then, with the optimized $\boldsymbol{Q}$, we update the transmit powers $\{p_1[n]\}_{n=1}^N$ during the first stage as $p_1[n]=q_1^2[n],\ \forall n\in\mathcal{N}$.

Algorithm 1: Proposed Algorithm for Problem (15)

1. Initialize $\boldsymbol{U}$, $\boldsymbol{P}$, and set $l=0$;
2. **repeat**
3. Set $l=l+1$;
4. Given $\boldsymbol{U}^{(l-1)}$ and $\boldsymbol{P}^{(l-1)}$, calculate $\boldsymbol{T}^{(l)}$ according to (17);
5. Given $\boldsymbol{T}^{(l)}$, update $\boldsymbol{U}^{(l)}$ and $\boldsymbol{P}^{(l)}$ by solving problem (39);
6. **until** *convergence*;
7. Return the optimal time durations $\boldsymbol{T}^*$, and the optimal trajectory $\boldsymbol{U}^*$ and transmit powers $\boldsymbol{P}^*$ of the UAV.

In summary, the original non-convex optimization problem in (15) is tackled in an alternating manner, by iteratively invoking the closed-form solution in (17) for the time duration optimization and solving the problem in (39) for the UAV's power and trajectory optimization. We summarize the iterative joint optimization algorithm in Algorithm 1.

C. Convergence and Complexity Analysis

For Algorithm 1, it can be verified that the objective value of the total energy consumption is non-increasing over the iterations and it must have a finite lower bound. Thus, the proposed algorithm is guaranteed to converge.

Moreover, the computational cost of Algorithm 1 mainly lies in iteratively updating $\boldsymbol{T}$ and solving (39). In particular, in each iteration, the complexity of updating $\boldsymbol{T}$ with the closed-form expression in (17) is given by $\mathcal{O}(KN)$. As for solving (39), according to the works in [30], [39] and [41], the complexity is given by $\mathcal{O}(K^3N^3)$.

IV. Numerical Results

In this part, we provide numerical results to evaluate the performance of the proposed algorithm.

A. Parameter Setup

We consider a UAV-enabled WPT and communication network consisting of a BS, a fixed-wing UAV, and $K=4$ users. The positions of the users and the BS are fixed and the users are located far way from the BS, such that the communication process between them needs to be accomplished with the assistance of the UAV. Without loss of generality, we assume that the BS is horizontally located at (100 m, 0 m) and the users are distributed on the vertexes of a square with coordinates (0 m, 0 m), (8 m, 0 m), (8 m, 8 m), and (0 m, 8 m), respectively, as depicted in Fig. 2. The transmission requirements of the four users are set to $\boldsymbol{r}=[r_1,r_2,r_3,r_4]=[6,8,8,4]$ Mbits. During the first stage, the initial point of the UAV's trajectory is set to $\boldsymbol{u}_0=$ (0 m, 8 m). Other specific values of the simulation parameters are presented in Table I.

This article has been accepted for publication in a future issue of this journal, but has not been fully edited. Content may change prior to final publication. Citation information: DOI10.1109/JIOT.2023.3281584, IEEE Internet of Things Journal

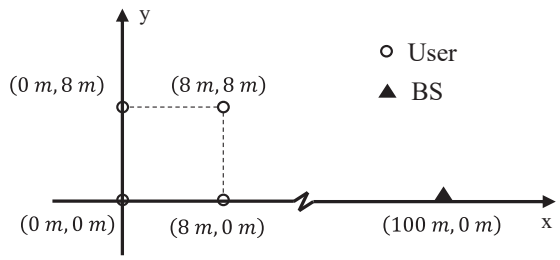

Fig. 2. Simulation setup.

TABLE I
SIMULATION PARAMETERS

Notation	Parameter	Value
B	Bandwidth	1 MHz
L	Number of antennas at the BS	4
M	Mass of the UAV	9.65 kg
N	Number of time intervals	30
$P_{\max}$	Maximum transmit power for WPT	50 dBm
P_c	Propulsion power of uniform circular flight	43 dBm
P_k	Transmit power of each user	10 dBm
$V_{\max}$	Maximum flight speed of the UAV	10 m/s
$V_{\min}$	Minimum flight speed of the UAV	1 m/s
η	Energy harvesting efficiency	0.9
H	Flight altitude of the UAV	10 m
D	Distance between the UAV and the BS	15 m
α_0	Reference channel power at $d_0 = 1$ m	-20 dB
σ^2	Noise power	-70 dBm

B. Benchmark Schemes

In order to validate the performance obtained by the proposed algorithm, we consider the following two benchmark schemes for comparisons.

- *Fly-hover-communicate:* We consider the popular fly-hover-communicate strategy [36], [37] as the first benchmark scheme. Specifically, the task of WPT and data collection in the first stage is completed in K continuous substages. During the k-th substage, the UAV flies to a position close to the k-th user and then the UAV hovers and transfers energy while the user transmits data. After that, the UAV proceeds with the next substage to serve user $k+1$. In particular, to increase the WPT efficiency, the UAV stays stably at point $\boldsymbol{u}_k = (x_k, y_k, H)$ when serving user k [37], where the charging power and duration are determined to minimize the corresponding energy consumption under the QoS constraint of user k. In addition, a constant speed $V = 3$ m/s is adopted when the UAV flies from $\boldsymbol{u}_k$ to $\boldsymbol{u}_{k+1}$.
- *Fixed trajectory:* Similarly to the previous works [24], [39], we additionally consider a benchmark scheme with fixed UAV trajectory. Since user 1, user 2, and user 3 have higher data transmission requirements, we assume that the UAV flies along a semi-circle trajectory from $\boldsymbol{u}_0$ with a radius of 4 m (as shown in Fig. 4), which is closer to these three users to better fulfill their transmission requirements.

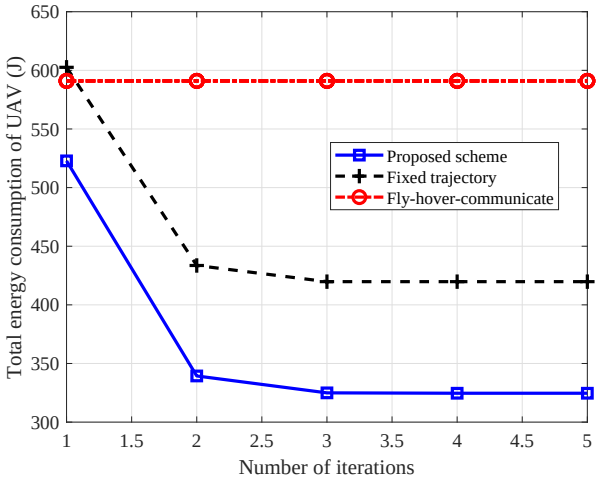

Fig. 3. Total energy consumptions of different schemes versus the number of iterations.

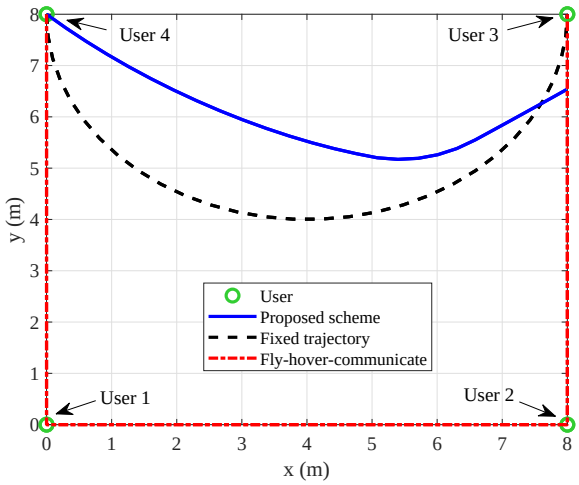

Fig. 4. Optimized trajectory and benchmark trajectories.

C. Simulation Results

Fig. 3 illustrates the convergence behaviours of different schemes. First, it is seen that both the proposed scheme and the fixed trajectory scheme converge within several iterations, while the performance of the non-iterative fly-hover-communicate scheme remains the same. Second, when the convergence is reached, the energy consumptions of the proposed and fixed trajectory schemes are much lower than that of the benchmark fly-hover-communicate scheme, due to the more flexible mobility of the UAV. Finally, compared to the scheme with fixed trajectory, the proposed scheme saves 23% energy, which validates its effectiveness.

Fig. 4 shows the UAV's flying trajectories during the first stage obtained in different schemes. The UAV flies from the specified initial location $\boldsymbol{u}_0 = (0\text{ m}, 8\text{ m})$ while keeping charging the users and collecting users' data along the flight. As discussed in the previous subsection, to increase the WPT efficiency, the UAV in the fly-hover-communicate scheme hovers above the grounds users successively and flies along

This article has been accepted for publication in a future issue of this journal, but has not been fully edited. Content may change prior to final publication. Citation information: DOI10.1109/JIOT.2023.3281584, IEEE Internet of Things Journal

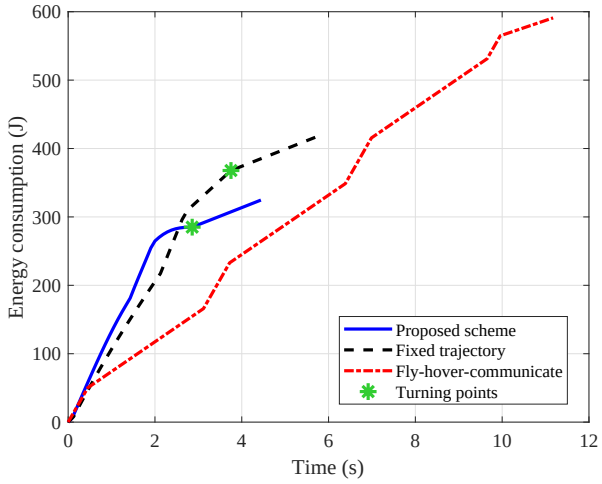

Fig. 5. Cumulative energy consumed by the UAV over time.

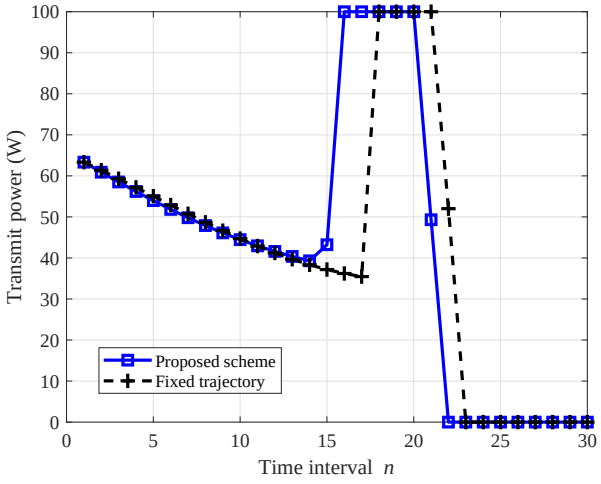

Fig. 7. Optimized charging powers in different time intervals.

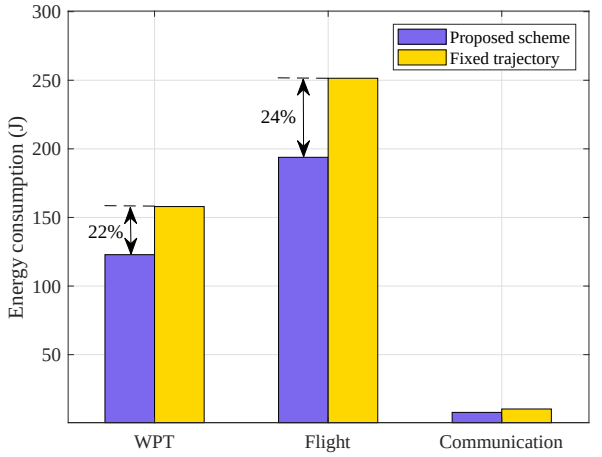

Fig. 6. Specific energy consumptions for WPT, flight, and communication.

the straight trajectories among these hovering positions. Under the proposed scheme, the optimized trajectory is a curve biased towards user 2. This is because user 2 has the highest data communication requirement, such that the UAV will fly closer to it to facilitate the fulfillment of the QoS constraints. Different from our proposed scheme, the trajectories of two benchmark schemes are not biased towards any users.

The cumulative energy consumed by the UAV over time is shown in Fig. 5. First, we can see that the fly-hover-communicate scheme has the longest transmission period with the highest energy consumption, as it is a simple baseline strategy with low design complexity. Then, focusing on the other two curves, we can observe that in the proposed scheme both the total time length and the total energy consumption are lower than those of the fixed trajectory scheme. This verifies the effectiveness of the proposed algorithm. In addition, the average slope in the first stage of these two curves is larger than that in the second stage. This is because the UAV needs to transfer energy to the users at stage 1, yielding a higher transmission power. Moreover, compared to the fixed trajectory scheme, although our proposed algorithm has a higher average power, the time length of stage 1, the length of the entire mission, and the total energy consumption are significantly reduced.

To show more details, in Fig. 6 we compare separately the specific energy consumptions for WPT, flight, and communication of the proposed scheme and the fixed trajectory scheme. Specifically, it is found that our proposed algorithm saves 22% and 24% energy from the perspectives of WPT and flight compared to the fixed trajectory scheme, respectively. Fig. 7 illustrates the optimized charging power during the first stage in different time intervals. It is found that at the first half of stage 1, a relatively medium and decreasing power is adopted to charge the users. When the time interval n gets larger than 15, the UAV works in full-power transmission, since at this time the UAV is located at the position with the highest average WPT efficiency for four users. Consequently, at the end of the first stage the UAV no longer charges users since the harvested energy at the users is sufficient for completing the remaining uplink data transmission.

Finally, we show the impacts of the communication requirements at the users. Specifically, we illustrate the total energy consumed by the UAV versus the increasing data requirements $\boldsymbol{r}' \triangleq \xi \boldsymbol{r}$ in Fig. 8. First, it is seen that our proposed scheme significantly outperforms two benchmark schemes under different ξ. In addition, with the increase of ξ, the total energy consumptions of all three schemes get larger. This is because more energy is needed to be transferred at the UAV to ensure that the harvested energy at the users can still guarantee the more stringent communication requirements.

V. Conclusion

We investigated a UAV-enabled energy harvesting and relaying network. The UAV not only serves as a wireless power transmission source, but also acts as an uplink relay to forward users' data to the BS. We jointly optimized the time durations and the corresponding UAV's transmit powers and trajectory of the system to minimize the total energy consumption at

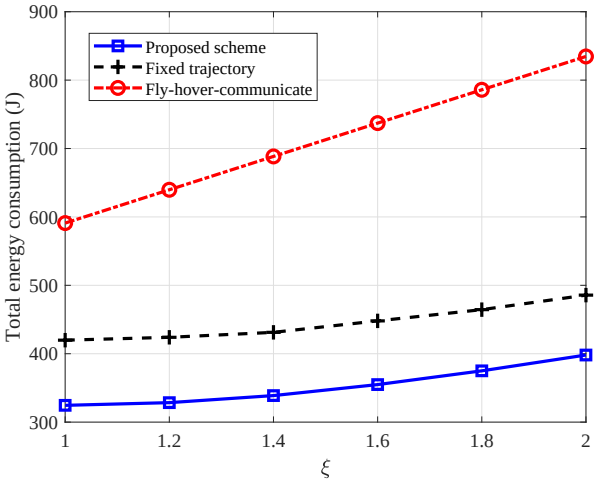

Fig. 8. Total energy consumed by the UAV versus the increasing data communication requirements $\boldsymbol{r}' \triangleq \xi \boldsymbol{r}$, with ξ increasing from 1 to 2.

the UAV. An efficient iterative algorithm was proposed to tackle the original highly intractable non-convex problem by decomposing it into two subproblems and solving them alternatingly. Simulation results verified that the algorithm only takes a few number of iterations to converge and outperforms the benchmark schemes.

Appendix A
Proof of Proposition 1

It is observed that the decision variable t_2 is involved in the objective function and the second constraint. Moreover, since the objective function is monotonically increasing with respect to t_2, it follows that the second inequality constraint must keep active at the optimality, which can be proved by contradiction. In other words, the optimal solution with respect to t_2 obeys

$$t_2^* = \frac{\sum_{k=1}^{K}\sum_{n=1}^{N} R_k[n]}{R_{ub}NK} t_1^*. \tag{40}$$

Consequently, substituting (40) into (16) yields a new problem with respect to t_1, which is given by

$$\begin{aligned} \underset{t_1 \geq 0}{\text{minimize}} \quad & \left(\bar{p}_1 + \frac{p_2 + P_{\mathrm{c}}}{R_{ub}NK}\sum_{k=1}^{K}\sum_{n=1}^{N} R_k[n]\right) t_1 \\ & + \sum_{n=1}^{N-1} \frac{0.5MN}{t_1} \|\boldsymbol{u}[n+1] - \boldsymbol{u}[n]\|^2 \\ \text{subject to} \quad & \sum_{n=1}^{N} R_k[n] \frac{t_1}{NK} \geq r_k, \ \forall k \in \mathcal{K}, \\ & V_{\min} \leq \frac{\|\boldsymbol{u}[n+1] - \boldsymbol{u}[n]\|}{t_1/N} \leq V_{\max}, \\ & n = 1, \cdots, N-1. \end{aligned} \tag{41}$$

In what follows, we discuss the solution to problem (41).

To begin with, we first determine the feasible range of t_1 by manipulating the linear constraints of problem (41). Specifically, we rearrange the first set of constraints in (41) and obtain the following restriction of t_1 as

$$t_1 \geq \underset{\forall k \in \mathcal{K}}{\text{maximize}} \quad \frac{r_k KN}{\sum_{n=1}^{N} R_k[n]} \triangleq \mathrm{lb}_0. \tag{42}$$

Then, the set of flight speed constraints is equivalent to

$$t_1 \geq \frac{\|\boldsymbol{u}[n+1] - \boldsymbol{u}[n]\| N}{V_{\max}} \triangleq \mathrm{lb}_n, \tag{43}$$

$$t_1 \leq \frac{\|\boldsymbol{u}[n+1] - \boldsymbol{u}[n]\| N}{V_{\min}} \triangleq \mathrm{ub}_n, \tag{44}$$

for $n = 1, \cdots, N-1$. Combining these results, the feasible range of t_1 can be expressed as $t_1 \in [\min_{t_1}, \max_{t_1}]$, where $\min_{t_1} = \max(\mathrm{lb}_0, \mathrm{lb}_1, \cdots, \mathrm{lb}_{N-1})$ and $\max_{t_1} = \min(\mathrm{ub}_1, \cdots, \mathrm{ub}_{N-1})$.

Next, we pay our attention to the objective function of (41), which is defined by $f(t_1)$ to simplify the presentation. The first-order derivative of $f(t_1)$ is calculated as

$$\begin{aligned} f'(t_1) = \bar{p}_1 + \frac{p_2 + P_{\mathrm{c}}}{R_{ub}NK}\sum_{k=1}^{K}\sum_{n=1}^{N} R_k[n] \\ - \frac{0.5MN}{t_1^2}\sum_{n=1}^{N-1} \|\boldsymbol{u}[n+1] - \boldsymbol{u}[n]\|^2. \end{aligned} \tag{45}$$

By letting $f'(t_1) = 0$, it is straightforward to acquire the unique positive stationary point of $f(t_1)$ by

$$\tilde{t}_1 = \sqrt{\frac{MN\sum_{n=1}^{N-1} \|\boldsymbol{u}[n+1] - \boldsymbol{u}[n]\|^2}{2\left(\bar{p}_1 + \frac{p_2+P_{\mathrm{c}}}{R_{ub}NK}\sum_{k=1}^{K}\sum_{n=1}^{N} R_k[n]\right)}}. \tag{46}$$

Moreover, it follows that $f'(t_1) > 0$ when $t_1 > \tilde{t}_1$ and $f'(t_1) < 0$ when $t_1 < \tilde{t}_1$. This admits that $f(t_1)$ is monotonically decreasing and increasing over $t_1 \in (0, \tilde{t}_1)$ and $t_1 \in (\tilde{t}_1, +\infty)$, respectively, i.e., $t_1 = \tilde{t}_1$ is the unique minimizer of $f(t_1)$ for $t_1 > 0$.

Based on the obtained equivalent feasible range and the first-order optimality property of the objective function, we finally arrive at the closed-form solution of (16) as shown in (17).

References

[1] P. Kamalinejad, C. Mahapatra, Z. Sheng, S. Mirabbasi, V. C. M. Leung, and Y. L. Guan, "Wireless energy harvesting for the Internet of Things," *IEEE Commun. Mag.*, vol. 53, no. 6, pp. 102–108, Jun. 2015.

[2] Z. Sheng, S. Yang, Y. Yu, A. V. Vasilakos, J. A. Mccann, and K. K. Leung, "A survey on the IETF protocol suite for the Internet of Things: Standards, challenges, and opportunities," *IEEE Wireless Commun.*, vol. 20, no. 6, pp. 91–98, Dec. 2013.

[3] W. Xu, Z. Yang, D. W. K. Ng, M. Levorato, Y. C. Eldar, and M. Debbah, "Edge learning for B5G networks with distributed signal processing: Semantic communication, edge computing, and wireless sensing," *IEEE J. Sel. Topics Signal Process.*, vol. 17, no. 1, pp. 9–39, Jan. 2023.

[4] W. Shi, W. Xu, X. You, C. Zhao and K. Wei, "Intelligent reflection enabling technologies for integrated and green Internet-of-Everything beyond 5G: Communication, sensing, and security," *IEEE Wireless Commun.*, vol. 30, no. 2, pp. 147–154, Apr. 2023.

[5] A. Al-Fuqaha, M. Guizani, M. Mohammadi, M. Aledhari, and M. Ayyash, "Internet of Things: A survey on enabling technologies, protocols, and applications," *IEEE Commun. Surveys Tuts.*, vol. 17, no. 4, pp. 2347–2376, 4th Quart., 2015.

[6] S. Sudevalayam and P. Kulkarni, "Energy harvesting sensor nodes: Survey and implications," *IEEE Commun. Surveys Tuts.*, vol. 13, no. 3, pp. 443–461, Sep. 2011.

[7] S. Bi, C. K. Ho, and R. Zhang, "Wireless powered communication: Opportunities and challenges," *IEEE Commun. Mag.*, vol. 53, no. 4, pp. 117–125, Apr. 2015.

[8] R. Zhang and C. K. Ho, "MIMO broadcasting for simultaneous wireless information and power transfer," *IEEE Trans. Wireless Commun.*, vol. 12, no. 5, pp. 1989–2001, May 2013.

[9] G. Yang, C. K. Ho, and Y. L. Guan, "Dynamic resource allocation for multiple-antenna wireless power transfer," *IEEE Trans. Signal Process*, vol. 62, no. 14, pp. 3565–3577, Jul. 2014.

[10] B. Clerckx, R. Zhang, R. Schober, D. W. K. Ng, D. I. Kim, and H. V. Poor, "Fundamentals of wireless information and power transfer: From RF energy harvester models to signal and system designs," *IEEE J. Sel. Areas Commun.*, vol. 37, no. 1, pp. 4–33, Jan. 2019.

[11] J. Xu, Y. Zeng, and R. Zhang, "UAV-enabled wireless power transfer: Trajectory design and energy optimization," *IEEE Trans. Wireless Commun.*, vol. 17, no. 8, pp. 5092–5106, Aug. 2018.

[12] C. Xiong, G. Y. Li, S. Zhang, Y. Chen, and S. Xu, "Energy- and spectral-efficiency tradeoff in downlink OFDMA networks", *IEEE Trans. Wireless Commun.*, vol. 10, no. 11, pp. 3874–3886, Nov. 2011.

[13] W. Xu, Y. Cui, H. Zhang, G. Li, and X. You, "Robust beamforming with partial channel state information for energy efficient networks," *IEEE J. Sel. Areas Commun.*, vol. 33, no. 12, pp. 2920–2935, Dec. 2015.

[14] Z. He, W. Xu, H. Shen, Y. Huang, and H. Xiao, "Energy efficient beamforming optimization for integrated sensing and communication," *IEEE Wireless Commun. Lett.*, vol. 11, no. 7, pp. 1374–1378, Jul. 2022.

[15] J. Xu, L. Liu, and R. Zhang, "Multiuser MISO beamforming for simultaneous wireless information and power transfer," *IEEE Trans. Signal Process.*, vol. 62, no. 18, pp. 4798–4810, Sep. 2014.

[16] G. Yang, C. K. Ho, R. Zhang, and Y. L. Guan, "Throughput optimization for massive MIMO systems powered by wireless energy transfer," *IEEE J. Sel. Areas Commun.*, vol. 33, no. 8, pp. 1640–1650, Aug. 2015.

[17] G. Amarasuriya, E. G. Larsson, and H. V. Poor, "Wireless information and power transfer in multiway massive MIMO relay networks," *IEEE Trans. Wireless Commun.*, vol. 15, no. 6, pp. 3837–3855, Jun. 2016.

[18] F. Wang, J. Xu, X. Wang, and S. Cui, "Joint offloading and computing optimization in wireless powered mobile-edge computing systems," *IEEE Trans. Wireless Commun.*, vol. 17, no. 3, pp. 1784–1797, Mar. 2018.

[19] M. Xia and S. Aissa, "On the efficiency of far-field wireless power transfer," *IEEE Trans. Signal Process.*, vol. 63, no. 11, pp. 2835–2847, Jun. 2015.

[20] S. Bi and R. Zhang, "Distributed charging control in broadband wireless power transfer networks," *IEEE J. Sel. Areas Commun.*, vol. 34, no. 12, pp. 3380–3393, Dec. 2016.

[21] Y. Zeng, R. Zhang, and T. J. Lim, "Wireless communications with unmanned aerial vehicles: Opportunities and challenges," *IEEE Commun. Mag.*, vol. 54, no. 5, pp. 36–42, May 2016.

[22] N. Zhao *et al.*, "UAV-assisted emergency networks in disasters," *IEEE Wireless Commun.*, vol. 26, no. 1, pp. 45–51, Feb. 2019.

[23] Q. Hu, Y. Cai, G. Yu, Z. Qin, M. Zhao, and G. Y. Li, "Joint offloading and trajectory design for UAV-enabled mobile edge computing systems," *IEEE Internet Things J.*, vol. 6, no. 2, pp. 1879–1892, Apr. 2019.

[24] J. Zhang, L. Zhou, Q. Tang, E. C. Ngai, X. Hu, H. Zhao, and J. Wei, "Stochastic computation offloading and trajectory scheduling for UAV-assisted mobile edge computing," *IEEE Internet Things J.*, vol. 6, no. 2, pp. 3688–3699, Apr. 2019.

[25] W. Lu *et al.*, "Resource and trajectory optimization for secure communications in dual-UAV-MEC systems," *IEEE Trans. Ind. Informat.*, vol. 18, no. 4, pp. 2704–2713, Apr. 2022.

[26] F. Ono, H. Ochiai, and R. Miura, "A wireless relay network based on unmanned aircraft system with rate optimization," *IEEE Trans. Wireless Commun.*, vol. 15, no. 11, pp. 7699–7708, Nov. 2016.

[27] Y. Zeng, R. Zhang, and T. J. Lim, "Throughput maximization for UAV-enabled mobile relaying systems," *IEEE Trans. Commun.*, vol. 64, no. 12, pp. 4983–4996, Dec. 2016.

[28] S. Zhang, H. Zhang, Q. He, K. Bian, and L. Song, "Joint trajectory and power optimization for UAV relay networks," *IEEE Commun. Lett.*, vol. 22, no. 1, pp. 161–164, Jan. 2018.

[29] C. Pan, H. Ren, Y. Deng, M. Elkashlan, and A. Nallanathan, "Joint blocklength and location optimization for URLLC-enabled UAV relay systems," *IEEE Wireless Commun. Lett.*, vol. 23, no. 3, pp. 498–501, Mar. 2019.

[30] Y. Ji, Z. Yang, H. Shen, W. Xu, K. Wang, and X. Dong, "Multicell edge coverage enhancement using mobile UAV-relay," *IEEE Internet Things J.*, vol. 7, no. 8, pp. 7482–7494, Aug. 2020.

[31] F. Cheng *et al.*, "UAV trajectory optimization for data offloading at the edge of multiple cells," *IEEE Trans. Veh. Technol.*, vol. 67, no. 7, pp. 6732–6736, Jul. 2018.

[32] Q. Zhang, M. Jiang, Z. Feng, W. Li, W. Zhang, and M. Pan, "IoT enabled UAV: Network architecture and routing algorithm," *IEEE Internet Things J.*, vol. 6, no. 2, pp. 3727–3742, Apr. 2019.

[33] Q. Yuan, Y. Hu, C. Wang, and Y. Li, "Joint 3D beamforming and trajectory design for UAV-enabled mobile relaying system," *IEEE Access*, vol. 7, pp. 26488–26496, Feb. 2019.

[34] Y. Hu, X. Yuan, J. Xu, and A. Schmeink, "Optimal 1D trajectory design for UAV-enabled multiuser wireless power transfer," *IEEE Trans. Commun.*, vol. 67, no. 8, pp. 5674–5688, Aug. 2019.

[35] X. Yuan, Y. Hu, and A. Schmeink, "Joint design of UAV trajectory and directional antenna orientation in UAV-enabled wireless power transfer networks," *IEEE J. Sel. Areas Commun.*, vol. 39, no. 10, pp. 3081–3096, Oct. 2021.

[36] L. Xie, J. Xu, and R. Zhang, "Throughput maximization for UAV-enabled wireless powered communication networks," *IEEE Internet Things J.*, vol. 6, no. 2, pp. 1690–1703, Apr. 2019.

[37] Z. Yang, W. Xu, and M. Shikh-Bahaei, "Energy efficient UAV communication with energy harvesting," *IEEE Trans. Veh. Technol.*, vol. 69, no. 2, pp. 1913–1927, Feb. 2020.

[38] X. Lu, W. Yang, S. Yan, Z. Li, and D. W. K. Ng, "Covertness and timeliness of data collection in UAV-aided wireless-powered IoT," *IEEE Internet Things J.*, vol. 9, no. 14, pp. 12573–12587, Jul. 2022.

[39] F. Zhou, Y. Wu, R. Q. Hu, and Y. Qian, "Computation rate maximization in UAV-enabled wireless-powered mobile-edge computing systems," *IEEE J. Sel. Areas Commun.*, vol. 36, no. 9, pp. 1927–1941, Sep. 2018.

[40] F. Zhou, Y. Wu, H. Sun, and Z. Chu, "UAV-enabled mobile edge computing: Offloading optimization and trajectory design," in *Proc. IEEE Int. Conf. Commun. (ICC)*, Kansas City, MO, USA, May 2018, pp. 1–6.

[41] S. Boyd and L. Vandenberghe, *Convex Optimization*. Cambridge, U. K.: Cambridge Univ. Press, 2004.

[42] M. Grant and S. Boyd. (Dec. 2018). *CVX: MATLAB Software for Disciplined Convex Programming.* [Online]. Available: http://cvxr.com/cvx/

[43] T. Lipp and S. Boyd, "Variations and extension of the convex-concave procedure," *Optim. Eng.*, vol. 17, no. 2, pp. 263–278, Jun. 2016.

Zhenyao He (Graduate Student Member, IEEE) received the B.E. degree in information engineering and the M.S. degree in information and communication engineering from Southeast University, Nanjing, China, in 2018, 2020, respectively, where he is currently pursuing the Ph.D. degree with the National Mobile Communications Research Laboratory. His research interests include MIMO communications and integrated sensing and communications.

Yukuan Ji received the M.S. degree in information and communication engineering with the School of Information Science and Engineering, Southeast University, Nanjing, China, in 2020. She is currently an assistant engineer with Nanjing Power Supply Company, State Grid Jiangsu Electric Power Company Ltd. Her research interests include 5G mobile communication, power grids, UAV communication, and optical fiber communication.

Kezhi Wang (Senior Member, IEEE) received the Ph.D. degree in engineering from the University of Warwick, U.K. He was with the University of Essex and Northumbria University, U.K. Currently, he is a Senior Lecturer with the Department of Computer Science, Brunel University London, U.K. His research interests include wireless communications, mobile edge computing, and machine learning.

Wei Xu (Senior Member, IEEE) received his B.Sc. degree in electrical engineering and his M.S. and Ph.D. degrees in communication and information engineering from Southeast University, Nanjing, China in 2003, 2006, and 2009, respectively. Between 2009 and 2010, he was a Post-Doctoral Research Fellow at the University of Victoria, Canada. He was an Adjunct Professor of the University of Victoria in Canada from 2017 to 2020, and a Distinguished Visiting Fellow of the Royal Academy of Engineering, U.K. in 2019. He is currently a Professor at Southeast University. His research interests include information theory, signal processing, and machine learning for wireless communications.

Dr. Xu received the Youth Science and Technology Award of China Institute of Communications in 2018, the Science and Technology Award of the Chinese Institute of Electronics (Second Prize) in 2019, the National Natural Science Foundation of China for Outstanding Young Scholars in 2020, the IEEE Communications Society Heinrich Hertz Award in 2023, and the Best Paper Awards at IEEE Globecom 2014, IEEE ICCC 2014, ISWCS 2018, and WCSP 2017, 2021. He served as an Editor of IEEE COMMUNICATIONS LETTERS from 2012 to 2017, and an Editor of IEEE TRANSACTIONS ON COMMUNICATIONS from 2018 to 2023. He is a Senior Editor of IEEE COMMUNICATIONS LETTERS. He is a Fellow of IET.

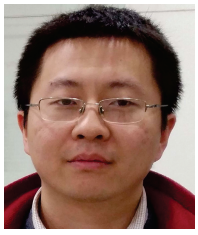

Hong Shen (Member, IEEE) received the B.E., M.S., and Ph.D. degrees in information and communication engineering from Southeast University, Nanjing, China, in 2009, 2011, and 2014, respectively. During his doctoral studies, he has conducted cooperative research with the Department of Electrical and Computer Engineering, University of California at Davis, Davis, CA, USA. He is currently an Associate Professor with the National Mobile Communications Research Laboratory, Southeast University. His research interests include integrated sensing and communications, deep learning aided communications, and short packet communications.

Ning Wang (Member, IEEE) received the B.E. degree in communication engineering from Tianjin University, China, in 2004, the M.A.Sc. degree in electrical engineering from The University of British Columbia, Canada, in 2010, and the Ph.D. degree in electrical engineering from the University of Victoria, Canada, in 2013. From 2004 to 2008, he was with the China Information Technology Design and Consulting Institute as a Mobile Communication System Engineer, specializing in planning and optimization of commercial mobile communication networks. From 2013 to 2015, he was a Postdoctoral Research Fellow with the Department of Electrical and Computer Engineering, The University of British Columbia. Since 2015, he has been with the School of Information Engineering, Zhengzhou University, Zhengzhou, China, where he is currently a Professor. He also holds adjunct appointments with the Department of Electrical and Computer Engineering, McMaster University, Canada, and the State Key Laboratory of Millimeter Waves, Southeast University, China. His research interests include resource allocation and security designs of future cellular networks, channel modeling for wireless communications, statistical signal processing, and cooperative wireless communications. He was on the technical program committees of international conferences, including the IEEE GLOBECOM, IEEE ICC, IEEE WCNC, and CyberC.

Xiaohu You (Fellow, IEEE) received the M.S. and Ph.D. degrees in electrical engineering from Southeast University, Nanjing, China, in 1985 and 1988, respectively. Since 1990, he has been with the National Mobile Communications Research Laboratory, Southeast University, where he is currently the Director and a Professor. From 1999 to 2002, he was a Principal Expert of the C3G Project, responsible for organizing Chinas 3G Mobile Communications Research and Development Activities. From 2001 to 2006, he was a Principal Expert of the China National 863 Beyond 3G FuTURE Project. Since 2013, he has been a Principal Investigator of the China National 863 5G Project. He has contributed over 200 IEEE journal articles and two books in the areas of adaptive signal processing and neural networks, and their applications to communication systems. His research interests include mobile communication systems, and signal processing and its applications.

Dr. You was selected as an IEEE Fellow for his contributions to the development of mobile communications in China in 2011. He was a recipient of the National 1st Class Invention Prize in 2011. He has served as the General Chair of the IEEE Wireless Communications and Networking Conference 2013, the IEEE Vehicular Technology Conference 2016, and the IEEE International Conference on Communications 2019. He is the Secretary-General of the FuTURE Forum and the Vice-Chair of the China IMT-2020 Promotion Group and the China National Mega Project on New Generation Mobile Network.